# Grating-based phase-contrast CT (PCCT): histopathological correlation of human liver cirrhosis and hepatocellular carcinoma specimen

Melanie A Kimm ,[1] Marian Willner,[2] Enken Drecoll,[3] Julia Herzen,[2] Peter B Noël,[1,4] Ernst J Rummeny,[1] Franz Pfeiffer,[2] Alexander A Fingerle[1]

[1]Department of Diagnostic and Interventional Radiology, School of Medicine & Klinikum rechts der Isar, Technical University of Munich, Munich, Germany
[2]Chair of Biomedical Physics, Department of Physics and Munich School of Bioengineering, Technical University of Munich, Garching , Germany
[3]Department of Pathology, School of Medicine & Technical University of Munich, Munich, Germany
[4]Department of Radiology, University of Pennsylvania, Philadelphia, Pennsylvania, USA

**Correspondence to**
Dr Melanie A Kimm, Department of diagnostic and interventional Radiology, Klinikum rechts der Isar der Technischen Universitat Muenchen, Munich, Germany; melanie.kimm@tum.de

Received 11 December 2019
Revised 16 December 2019
Accepted 17 December 2019
Published Online First 15 January 2020



**To cite:** Kimm MA, Willner M, Drecoll E, *et al*. *J Clin Pathol* 2020;**73**:483–487.

## ABSTRACT

**Aims** To correlate signal intensities in grating-based phase-contrast CT (PCCT) images obtained at a synchrotron light source and a conventional X-ray source with tissue components in human liver cirrhosis and hepatocellular carcinoma (HCC) specimen.

**Methods** Study approval was obtained by the institutional review board. Human specimen of liver cirrhosis and HCC were imaged at experimental grating-based PCCT setups using either a synchrotron radiation source or a conventional X-ray tube. Tissue samples were sectioned and processed for H&E and Elastica van Gieson staining. PCCT and histological images were manually correlated. Depending on morphology and staining characteristics tissue components like fibrosis, HCC, inflammation, connective tissue and necrosis were differentiated and visually correlated with signal intensity in PCCT images using a 5-point Likert scale with normal liver parenchyma as a reference.

**Results** Grating-based PCCT images of human cirrhotic liver and HCC specimen showed high soft-tissue contrast allowing correlation with histopathological sections. Signal intensities were similar in both setups independent of the nature of the radiation source. Connective tissue and areas of haemorrhage displayed the highest signal intensities, fibrotic liver tissue the lowest.

**Conclusions** Grating-based PCCT provides comparable results for the characterisation of human specimen of liver cirrhosis and HCC using either a synchrotron light source or a conventional X-ray tube. Due to its high soft-tissue contrast and its applicability to conventional X-ray tubes grating-based PCCT holds potential for preclinical research and virtual histology applications.

## INTRODUCTION

CT is widely regarded as one of the most important inventions in medical history. However, since the first installation of a CT scanner at the Kings College in London in 1972, the basic principle of image contrast formation in CT has remained unchanged. The attenuation of X-rays by the examined object serves as the sole source of contrast. A limiting factor of conventional CT is its low sensitivity to minor changes in linear attenuation coefficients with correspondingly low soft-tissue contrast. Thus, it can be challenging to detect and characterise diffuse parenchymal disease or focal lesions, for example, in the liver. Contrast media can improve soft-tissue contrast in conventional CT, nevertheless their intravenous application poses risks to some patient groups or may be contraindicated. Also, contrast media is not applicable to ex vivo imaging of tissue samples. In clinical imaging, CT is limited in the detection and delineation of early hepatocellular carcinoma (HCC), a tumour that develops in the majority of cases in patients with liver cirrhosis.[1] However, early detection and correct assessment of tumour stage are important for therapy and prognosis.

X-ray phase-contrast imaging is a novel imaging modality, which has been intensively studied over the last two decades. It has been shown that phase-contrast imaging provides superior soft-tissue contrast in comparison to conventional attenuation-based X-ray imaging.[1–4] By exploiting wave–optical interactions of the X-ray beam, advanced contrast modalities like phase-contrast and dark-field contrast can be obtained. Phase-contrast X-ray imaging has been achieved using different methods, most of them depending on highly brilliant synchrotron radiation limiting its application to a few research facilities worldwide.[5] However, a grating-based approach to phase-contrast imaging has been successfully translated to standard X-ray tubes[6 7] allowing integration into a small animal CT scanner.[8] Several recent publications have demonstrated the superior soft-tissue contrast of phase-contrast CT (PCCT) images compared with conventional attenuation-based CT images and the possibility to discriminate between certain tissue types. In ex vivo liver specimen, it has been shown that PCCT improves detectability of focal lesions and allows delineation of internal structures.[9 10] Through simultaneous assessment of the attenuation and phase-contrast signal PCCT allows the discrimination of different types of cystic renal lesions in an in vitro phantom.[11] Braunagel *et al* could differentiate soft-tissue components of renal cell carcinoma subtypes using qualitative and quantitative PCCT.[12] As PCCT is an emerging imaging modality, the knowledge about signal intensities of normal and pathological tissue components in PCCT images is limited. So far, qualitative and quantitative imaging features of PCCT have not been investigated in human liver cirrhosis and HCC. Therefore, the purpose of our study is to visually correlate signal intensities in PCCT images obtained at a synchrotron light source and a conventional X-ray source with tissue components of human liver cirrhosis and HCC specimen.

## MATERIAL AND METHODS

### Human liver specimen

Tissue samples for this retrospective study were acquired through the Department of Pathology at the University Hospital Klinikum rechts der Isar, Technical University of Munich.

The tissue samples S1 and S2 used in this study were parts from surgical specimen of two male patients (average age=60.5 years) who underwent curative partial hepatectomy for HCC. Sample S1 consists of cirrhotic liver tissue, sample S2 shows HCC.

### Grating-based PCCT setup

A detailed description of the imaging setup at the Deutsches Elektronen-Synchrotron (DESY) and the used laboratory setup can be found in Herzen *et al*[13] and Willner *et al*,[14] respectively.

The laboratory-based phase-contrast imaging system used for the experiments is located at the Technical University of Munich, Germany. It consists of a rotating molybdenum anode X-ray tube, a Talbot-Lau grating interferometer and a photon-counting detector (Pilatus II, Dectris, Switzerland). The three gratings employed in the interferometer were fabricated at the Karlsruhe Institute of Technology, Germany. All the gratings were made of gold with periods of 5.4 µm. Two of the gratings act as transmission gratings with structure heights of about 70 µm. They are installed behind the source and in front of the detector, respectively, with a distance of 170 cm between the two. A phase grating of 5.2 µm height is directly placed in the middle and introduces a phase shift of $\pi$ to X-rays of 27 keV. The rotation stage is mounted close to the phase grating providing a sample magnification of 1.7. This results in a field of view of $4\times2\,cm^2$ and an effective pixel size of $100\times100\,\mu m^2$. The phase stepping procedure required to extract the phase information is performed by a mechanical nanoconverter driven by a precision motorised actuator.

The synchrotron-based measurements were carried out at the synchrotron radiation wiggler source of the beamline W2 at the storage ring DORIS (DESY, Hamburg, Germany) using a Talbot grating interferometer. The interferometer consists of three optical gratings: the gold source grating with a period of 22.29 µm and a duty cycle of 0.6; the phase grating with a period of 4.33 µm; and the gold analyser grating with the period of 2.4 µm. The tomographic scans were performed in a water tank (made of PMMA (polymethylmethacrylate), 23 mm thickness of water in the beam direction) filled with demineralised water using 30 keV and the fifth Talbot order.

### Grating-based PCCT image acquisition and reconstruction

Sample S1 was imaged at the DESY (English German Electron Synchrotron) in Hamburg, Germany, and at an experimental laboratory PCCT setup using a conventional X-ray tube at the Chair of Biomedical Physics, Technical University of Munich in Garching, Germany. As both imaging setups provided similar signal intensities for the different tissue components, sample S2 was imaged only at the laboratory PCCT setup with the conventional X-ray tube. In both experiments, 1X Phosphate-buffered saline filled plastic cylinders (50 mL Corning Falcon tubes) containing the formalin fixed samples were submerged in a water bath to avoid phase-wrapping artefacts.

In brief, the tomographic scan at the laboratory setup included 800 projection images recorded with 11 phase steps and 3 s exposure time. The voltage of the rotating molybdenum anode X-ray source was set to 40 kV. An effective pixel size of 100 µm was realised covering a sample size of 3 cm.

For the tomography scan at the synchrotron radiation source, 1001 projections were collected over 360° were recorded with eight phase-steps over two periods of the grating G2 for each projection. Due to the limited field of view, the specimen was scanned in three height steps with enough overlap to combine the tomograms. The exposure time was in the range of 25 s per image, changing during the scan to correct for the decreasing ring current of DORIS (Double Ring Store, synchrotron facility DESY, Germany) . The images were taken with a binning factor of 2. The effective pixel size was determined by an automated focusing procedure to be 6.3 µm, the spatial resolution is estimated to 20 µm.

A filtered back-projection algorithm with Hilbert filter kernel was applied for the tomographic reconstruction of the final phase-contrast datasets obtained at both setups.

### Histopathological assessment of tissue samples

Human liver specimen were fixed in 4% neutral-buffered formalin overnight, embedded in paraffin and serial sections of 3 µm thickness were cut with a standard microtome (Leica, Germany). Sections were processed and stained for H&E and Elastica van Gieson (EvG) staining (Morphisto, Germany). H&E staining results in dark blue nuclei, cytoplasm in red and collagen in pale pink. EvG staining allows the detailed discrimination of the connective tissue with black nuclei, red collagen fibres and yellow cytoplasm. All stains were examined by a pathologist with more than 5 years of experience in liver pathology. Images were obtained at a Zeiss Imager 2 microscope and Axio Vision software (Zeiss, Germany).

### Visual evaluation of PCCT images

H&E and EvG stained sections were visually aligned to PCCT images using prominent image features. Different tissue components (bile ducts, connective tissue, fibrosis, HCC, haemorrhage, inflammation, liver parenchyma, necrosis and vessels) identified in the stained sections were then correlated with the signal intensities in the corresponding areas of the PCCT images. The signal intensities were visually graded on a 5-point Likert scale compared with normal liver parenchyma serving as a reference. Signal intensity was graded either lower (-), equal (o) or higher (+, ++ or +++) compared with normal liver tissue (S1) or fibrotic tissue (S2).

## RESULTS

### Liver cirrhosis specimen: imaging features and signal intensities in PCCT images obtained at a synchrotron light source

Figure 1 shows two tomographic PCCT images (figure 1A,B) of a liver cirrhosis specimen at different section levels demonstrating high soft-tissue contrast. In figure 1A, a vertically oriented band-like structure with high signal intensity is present in the centre of the image correlating with an area of connective tissue with vessels and lots of fibroblasts in the images of the EvG and H&E stains (figure 1C,E). A thin tubular structure surrounded by the connective tissue demarcates through lower signal intensity and represents a slightly bigger vessel (figure 1A). The left side of the tissue section consists of isolated parts of liver lobules with pronounced lymphocyte infiltrates and starting fibrosis (figure 1C,E). On the right side of the connective tissue strand, an inhomogeneous necrotic area partially with pyknotic cell nuclei and cell debris can be identified (figure 1C,E).

Figures 1 and 2 show tomographic (figure 1A,B; figure 2A,B) and histological (figure 1C–F; figure 2C–F) image analysis of

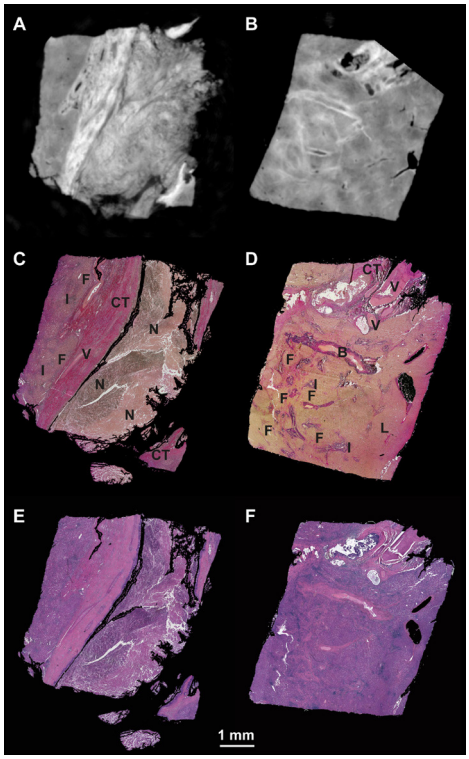


**Figure 1** Grating-based phase-contrast CT (PCCT) images of liver cirrhosis obtained at a synchrotron light source with correlation to histopathology (S1). PCCT images (A, B), Elastica van Gieson (EvG) stains (C, D) and H&E stains (E, F) of a liver cirrhosis specimen. Signal intensities in PCCT images (A, B) were correlated with corresponding areas in EvG and H&E stains (C, E and D, F, respectively). B, bile duct; CT, connective tissue; F, fibrosis; I, inflammation; L, liver parenchyma; n, necrosis; V, vessel.

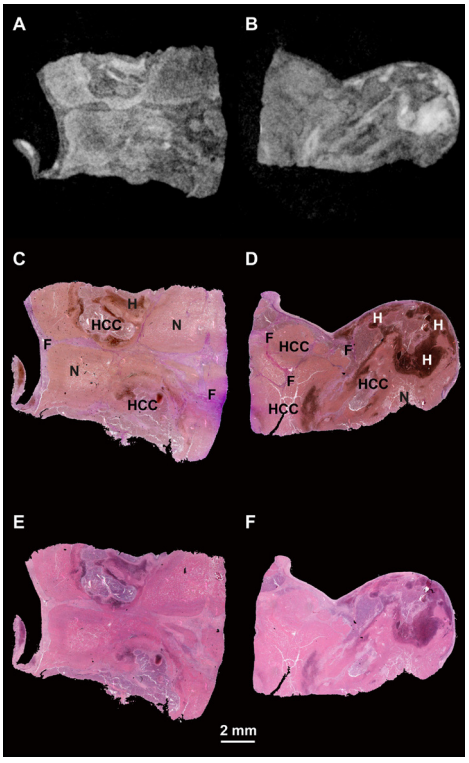


**Figure 2** Grating-based phase-contrast CT (PCCT) images of liver cirrhosis and hepatocellular carcinoma (HCC) obtained with a conventional X-ray tube with correlation to histopathology (S2). PCCT images (A, B), Elastica van Gieson (EvG) stains (C, D) and H&E stains (E, F) of HCC specimen. signal intensities in PCCT images (A, B) were correlated with corresponding areas in EvG and H&E stains (C, E and D, F, respectively). F, fibrosis; H, haemorrhage; HCC, hepatocellular carcinoma; n, necrosis.

dominant features of pathological liver specimen. We show in sample S1 (figure 1) fibrotic and cirrhotic areas with inhomogenous necrosis, respectively, in sample S2 (figure 2) a liver biopsy of a patient diagnosed with HCC. Fibrosis is characterised by the formation of excess fibrous connective tissue as a reparative response to injury or damage. HCC is besides others also characterised by nodules and infiltrations. Necrotic areas are an additional feature because of poor vascularisation. Depending on the remaining cell nuclei, the necrosis reflects different areas of perfusion.

In sample S1 (figure 1), histological analysis shows a strand of connective tissue in the middle of the image interspersed with vessels and lots of fibroblasts (figure 1C,E). Here, dense connective tissue results in a high signal intensity in the PCCT. Vessels within the connective tissue can be identified in the PCCT as darker signal and by their characteristic longitudinal structure. Fibrotic cells, however, do not lead to an intense signal change and are not well distinguishable from normal healthy liver tissue. Inflammatory infiltrations, however, as well as necrosis, in turn result in low to medium signal intensity in PCCT. Depending on the amount of pyknotic nuclei and vital cells, the signal varies slightly in its intensity. The loss of united cell structures is leading to a rougher structure in the CT image. Differences in signal intensities by the different histological features are also listed in table 1.

From the same specimen (S1) but approximately 0.5 mm above the just described area, we present a slide with fibrotic parts. In the H&E (figure 1F) and EvG (figure 1D) stain, a large bile duct with adjacent stroma and arterial and venous vessels can be identified. This part of the slide is again very prominent in the PCCT image (figure 1B) as the dense connective tissue around the duct and vessels leads to an increased signal intensity. Inflammatory processes visible specially around the bile ducts and also found to invade the surrounding liver tissue do give rise to a slight increase in signal intensity in the PCCT image. In both stains, H&E and EvG, leucocytes exhibit a high nucleus: cytoplasma ratio indicated by dark blue accumulations (figure 1D,F). In close proximity to the inflammatory processes, fibrotic areas can be found easily identified by its pinkish colour in the H&E and EvG stain. Nevertheless, the appearance of loose fibrotic

**Table 1** Signal intensities of different tissue types in liver cirrhosis in grating-based phase-contrast CT images obtained at a synchrotron light source

| | Signal intensity |
|---|---|
| Liver parenchyma (L) | Reference |
| Bile duct (B) | – |
| Connective tissue (CT) | +++ |
| Fibrosis (F) | o |
| Inflammation (I) | + |
| Necrosis (N) | ++ |
| Vessel (V) | – |

Visually assessed signal intensities compared with liver parenchyma: -, lower; o, equal; +/++/+++, higher.

**Table 2** Signal intensities of different tissue types in liver cirrhosis and hepatocellular carcinoma in grating-based phase-contrast CT images obtained with a conventional X-ray tube

| | Signal intensity |
|---|---|
| Fibrosis (F) | Reference |
| Hepatocellular carcinoma (HCC) | o/+ |
| Haemorrhage (H) | +++ |
| Necrosis (N) | + |

Visually assessed signal intensities compared with fibrosis: -, lower; o, equal; +/++/+++, higher.

cells within the tissue does not yet lead to increased signal intensity in PCCT. Only dense collagen rich connective tissue can be identified as white parts within the CT image. Leucocyte infiltration next to fibrotic areas are visualised by a blueish colour in both stains. We claim that the signal intensity in the fibrotic area of this slide is due to the accumulation of infiltrating leucocytes next to collagen rich vessels and only dense intact fibrotic cell structures lead to signal intensity in phase-contrast CT.

### HCC specimen: imaging features and signal intensities in PCCT images obtained with a conventional X-ray tube

The PCCT images of the second specimen S2 (figure 2A,B) containing HCC also show high soft-tissue contrast comparable to the images obtained at a synchrotron light source (figure 1A,B). However, as the image resolution is lower with the conventional X-ray tube setup, less details are visible. Correlation of signal intensities in PCCT images with different tissue components identified by EvG and H&E stains was nonetheless possible (figure 2C–F). PCCT signal intensities of different tissues components are listed in table 2. At both slice positions, the specimen is dominated by necrosis, haemorrhage and carcinoma cell infiltrates. In the EvG and H&E stains, fibrotic areas are clearly distinguishable due to the pinkish colour of the fibroblasts compared with the brownish necrotic parts (figure 2C–F). Similar to the results of the liver cirrhosis sample imaged at a synchrotron light source, fibrotic areas do not demonstrate increased signal intensity in PCCT images (figure 2A,B). By contrast, haemorrhages present in the right part of the EvG and H&E stain (figure 2D,F) are clearly visible in the PCCT image (figure 2B) due to very high signal intensities. Necrotic areas show a minor increase in signal intensity allowing delineation from regions of HCC and fibrosis with their slightly lower signal intensity in PCCT (figure 2A,B). In comparison to our imaging results of a liver cirrhosis sample at a synchrotron light source (figure 1, table 1), signal intensities in PCCT images obtained with a conventional X-ray tube setup show similar characteristics for different tissue types present in a HCC specimen (figure 2, table 2).

Our study shows for the first time that grating-based PCCT allows for detailed analysis of liver biopsies and even for the separation of distinct cellular tissue compositions. As no sectioning or staining is needed for grating-based PCCT, it will be a valuable additive for pathologists to examine biopsies.

## DISCUSSION

In this study, we performed visual correlation of signal intensities in PCCT images of a cirrhotic liver and an HCC specimen with histopathological tissue analysis. Our results demonstrate the high soft-tissue contrast of PCCT independent of the applied radiation source, which is consistent with previously published data (8, 9). The high-contrast PCCT images allow delineation of different tissue components as revealed by EvG and H&E stainings. Dense connective tissue and haemorrhage show highest signal intensities in PCCT images, followed by areas of necrosis. Protein-rich tissues have been shown to exhibit higher quantitative phase-contrast Hounsfield units (pHUs) compared with other tissue types[15] and human muscle tendons have demonstrated high signal intensity in PCCT images.[16] Since the type of connective tissue in our specimen contains large amounts of collagenous fibres, we observe comparable high signal intensities. Likewise, in a phantom study simulating cystic renal lesions, the amount of intracystic haemorrhage correlated with signal intensity in PCCT images and quantitative pHUs,[11] which is in agreement with our data showing high signal intensities in areas of focal haemorrhage. On the lower end, tubular structures like bile ducts and vessels classify with signal intensities below those of normal liver parenchyma. Overall, PCCT images allow for an identification and delineation of distinct tissue types in liver specimen. As no contrast agent or staining is needed, preclinical PCCT may have advantages over existing imaging techniques in pathology, like micro-CT, for the identification of relevant findings in resection specimen, previous to sectioning and histopathological staining.[17] Furthermore, three-dimensional reconstruction of whole slide histological data has shown value in the visualisation and diagnosis of disease.[18] Here, PCCT images with their high soft-tissue contrast may facilitate correlation with histopathological imagery. Currently, PCCT is limited to preclinical research and not available as a clinical imaging modality. However, X-ray dark-field radiography, a contrast modality extracting a different signal of phase-contrast imaging, has recently been adapted for lung imaging in human bodies.[19 20] In a clinical setting, PCCT has the potential to reduce application of contrast media and improve characterisation of liver lesions, due to its high soft-tissue contrast compared with conventional attenuation-based CT.

Our study has limitations. With only two liver specimen included in our experiments, the sample size is small. However, the conclusions drawn from our results show the high potential of this imaging application and investigations with different samples and larger sample sizes are in planning. We believe that the results will not be different, but refined.

Spatial resolution of PCCT is lower when using a conventional X-ray tube compared with a synchrotron radiation source, and this may limit application for tissue analysis. Our results show that tissue characterisation is feasible at both imaging setups and signal intensities for different tissue types is similar. In addition, using advanced imaging and reconstruction techniques, Viermetz *et al* significantly improved spatial resolution of grating-based PCCT using conventional X-ray sources.[21 22] We did not investigate the effect of formalin fixation on image contrast and signal intensities in PCCT. Yet, it has been demonstrated that formalin fixation does not degrade or artificially change image contrast and, therefore, is suitable for most biomedical phase-contrast imaging applications.[14]

### Take home messages

- X-ray phase-contrast imaging is a contrast-agent free imaging modality that allows soft-tissue characterisation ex vivo.
- Soft-tissue components like connective tissue, fibrosis and haemorrhage can be differentiated.
- Further studies are needed to refine the presented results.

In conclusion, with their high soft-tissue contrast, PCCT images allow visual characterisation of different tissue types in pathological human liver specimen based on characteristic signal intensities. Due to its applicability to conventional X-ray sources, grating-based PCCT holds potential for preclinical research and imaging applications in pathology.

**Handling editor** Runjan Chetty.

**Acknowledgements** We thank Peter Strzelczyk for technical support. The authors would like to thank the staff from the Helmholtz-Center Geesthacht of the W2 Beamline at DORIS (DESY, Hamburg) for technical support.

**Contributors** MAK, MW, ED, JH, PBN, FP and AAF designed the study. MAK, MW, ED, JH, PBN and AAF were responsible for data acquisition. Analysis and interpretation of data was performed by MAK, MW, ED, JH, PBN, EJR, FP and AAF. MAK and ED had full access to the histological data. MW, JH, PBN, FP and AAF had full access to the CT data in the study and take responsibility for the integrity of the data and the accuracy of the data analysis. All authors were involved in drafting the article or revising it critically for important intellectual content and all authors approved the final version to be published.

**Funding** Supported in part by the DFG Cluster of Excellence Munich-Centre for Advanced Photonics (MAP, DFG EXC-158) and the Center for Advanced Laser Applications (CALA).

**Competing interests** PBN reports grants from Philips Healthcare, outside the submitted work.

**Patient consent for publication** Not required.

**Ethics approval** The study was fully approved by the local ethics committee at the Faculty of Medicine of the Technical University of Munich (project number 4029/11).

**Provenance and peer review** Not commissioned; internally peer reviewed.

**Data availability statement** Data are available on reasonable request. The data are not publicly available due to them containing information that could compromise patient privacy.

**ORCID iD**
Melanie A Kimm http://orcid.org/0000-0001-6833-9738

## REFERENCES

1 Li J, Wang J, Lei L, *et al*. The diagnostic performance of gadoxetic acid disodium-enhanced magnetic resonance imaging and contrast-enhanced multi-detector computed tomography in detecting hepatocellular carcinoma: a meta-analysis of eight prospective studies. *Eur Radiol* 2019;29:6519–28.
2 Fitzgerald R. Phase-sensitive x-ray imaging. *Phys Today* 2000;53:23–6.
3 Pfeiffer F, Bunk O, David C, *et al*. High-resolution brain tumor visualization using three-dimensional X-ray phase contrast tomography. *Phys Med Biol* 2007;52:6923–30.
4 Pfeiffer F, Kottler C, Bunk O, *et al*. Hard X-ray phase tomography with low-brilliance sources. *Phys Rev Lett* 2007;98:108105.
5 Bravin A, Coan P, Suortti P. X-Ray phase-contrast imaging: from pre-clinical applications towards clinics. *Phys Med Biol* 2013;58:R1–35.
6 Bech M, Jensen TH, Feidenhans R, *et al*. Soft-Tissue phase-contrast tomography with an X-ray tube source. *Phys Med Biol* 2009;54:2747–53.
7 Pfeiffer F, Weitkamp T, Bunk O, *et al*. Phase retrieval and differential phase-contrast imaging with low-brilliance X-ray sources. *Nat Phys* 2006;2:258–61.
8 Tapfer A, Bech M, Velroyen A, *et al*. Experimental results from a preclinical X-ray phase-contrast CT scanner. *Proc Natl Acad Sci U S A* 2012;109:15691–6.
9 Herzen J, Willner MS, Fingerle AA, *et al*. Imaging liver lesions using Grating-Based phase-contrast computed tomography with Bi-Lateral filter post-processing. *PLoS One* 2014;9:e83369.
10 Noël PB, Herzen J, Fingerle AA, *et al*. Evaluation of the potential of phase-contrast computed tomography for improved visualization of cancerous human liver tissue. *Zeitschrift für Medizinische Physik* 2013;23:204–11.
11 Fingerle AA, Willner M, Herzen J, *et al*. Simulated cystic renal lesions: quantitative X-ray phase-contrast CT—An in vitro phantom study. *Radiology* 2014;272:739–48.
12 Braunagel M, Birnbacher L, Willner M, *et al*. Qualitative and quantitative imaging evaluation of renal cell carcinoma subtypes with Grating-based X-ray phase-contrast CT. *Sci Rep* 2017;7.
13 Herzen J, Donath T, Beckmann F, *et al*. X-Ray grating interferometer for materials-science imaging at a low-coherent wiggler source. *Rev Sci Instrum* 2011;82:113711.
14 Willner M, Fior G, Marschner M, *et al*. Phase-Contrast Hounsfield units of fixated and Non-Fixated soft-tissue samples. *PLoS One* 2015;10:e0137016.
15 Willner M, Viermetz M, Marschner M, *et al*. Quantitative three-dimensional imaging of lipid, protein, and water contents via X-ray phase-contrast tomography. *PLoS One* 2016;11:e0151889.
16 Donath T, Pfeiffer F, Bunk O, *et al*. Toward clinical X-ray phase-contrast CT: demonstration of enhanced soft-tissue contrast in human specimen.. *Invest Radiol* 2010;45:445–52.
17 Katsamenis OL, Olding M, Warner JA, *et al*. X-ray Micro-Computed tomography for nondestructive three-dimensional (3D) X-ray histology. *Am J Pathol* 2019;189:1608–20.
18 Fónyad L, Shinoda K, Farkash EA, *et al*. 3-dimensional digital reconstruction of the murine coronary system for the evaluation of chronic allograft vasculopathy. *Diagn Pathol* 2015;10:16.
19 Fingerle AA, De Marco F, Andrejewski J, *et al*. Imaging features in post-mortem X-ray dark-field chest radiographs and correlation with conventional X-ray and CT. *Eur Radiol Exp* 2019;3:25.
20 Willer K, Fingerle AA, Gromann LB, *et al*. X-ray dark-field imaging of the human lung-A feasibility study on a deceased body. *PLoS One* 2018;13:e0204565.
21 Birnbacher L, Viermetz M, Noichl W, *et al*. Tilted grating phase-contrast computed tomography using statistical iterative reconstruction. *Sci Rep* 2018;8:6608.
22 Viermetz M, Birnbacher L, Willner M, *et al*. High resolution laboratory grating-based X-ray phase-contrast CT. *Sci Rep* 2018;8:15884.